Selective Analytical Production of 1-Hydroxy-3,6-dioxabicyclo[3.2.1]octan-2-one from Catalytic Fast Pyrolysis of Cellulose with Zinc-Aluminium Layered Double Oxide Catalyst

Zhi-Bo Zhang, Qiang Lu,* Xiao-Ning Ye, Wen-Tao Li, Bin Hu, and Chang-Qing Dong *

Zinc-aluminium layered double oxide (Zn-Al-LDO) catalysts derived from layered double hydroxides (LDHs) were prepared and used for the catalytic fast pyrolysis of cellulose to selectively produce 1-hydroxy-3,6-dioxabicyclo[3.2.1]octan-2-one (LAC), which is a valuable anhydrosugar derivative. Analytical pyrolysis-gas chromatography/mass spectrometry (Py-GC/MS) experiments were performed to investigate the LAC production under different reaction conditions. The results indicated that the Zn-Al-LDO catalysts were capable of greatly inhibiting the pyrolytic formation of levoglucosan (LG) and capable of promoting the formation of LAC and certain other products. The catalyst with the Zn/Al molar ratio of 2 exhibited the best catalytic capacity for LAC production. Both pyrolysis temperature and the catalyst-to-cellulose ratio affected the pyrolytic product distribution remarkably. The maximal LAC yield was obtained at the pyrolysis temperature of 350 °C and catalyst-to-cellulose ratio of 4 and featured a peak area percentage of 21.9% (calculated by GC/MS), compared with only 3.0% from the non-catalytic process. In addition, the LDO catalyst performed better than the previously reported montmorillonite K-10 catalyst on the enhancement of LAC production.

Keywords: Cellulose; Catalytic fast pyrolysis; 1-Hydroxy-3,6-dioxabicyclo[3.2.1]octan-2-one; Py-GC/MS; Zinc-aluminium layered double oxide

Contact information: National Engineering Laboratory for Biomass Power Generation Equipment, North China Electric Power University, Beijing 102206, China;
**Corresponding authors: qianglu@mail.ustc.edu.cn; cqdong1@163.com*

INTRODUCTION

The fast pyrolysis of biomass offers a promising way to convert solid biomass into a liquid product known as bio-oil, which contains many valuable chemicals. The process known as selective fast pyrolysis of biomass has been widely investigated in recent years as a way of improving the pyrolytic selectivity towards target chemicals (Liu *et al.* 2014). Various methods have been developed to control the biomass pyrolysis process to obtain different valuable chemicals, mostly *via* the exploitation of catalysts. During the fast pyrolysis of cellulose or biomass, the depolymerization of cellulose produces various anhydrosugar and furan products, including LG, LAC, levoglucosenone (LGO), 1,5-anhydro-4-deoxy-D-glycero-hex-1-en-3-ulose (APP), 1,4:3,6-dianhydro-α-D- glucopyranose (DGP), 1,6-anhydro-β-D-glucofuranose (AGF), 5-hydroxymethyl furfural (HMF), 5-methyl furfural (MF), and furfural (FF). These compounds are all valuable chemicals. Their formation characteristics have been previously investigated (Lu *et al.* 2011b) and can be seen depicted in Fig. 1. Among these products of non-catalytic fast pyrolysis of cellulose,

LG is usually predominant (Lu *et al.* 2011b); thus, it can be easily produced with a high yield and high concentration (Zhuang *et al.* 2001). The other compounds are usually formed in lower yields and concentrations, because their formation pathways are difficult to be completed during conventional pyrolysis process (Shen and Gu 2009). Recently, the selective production of LGO and FF has been under wide investigation. Various acid catalysts, including H_3PO_4 (Dobele *et al.* 2003), H_2SO_4 (Sui *et al.* 2012), solid superacid (Lu *et al.* 2012), solid phosphoric acid (Zhang *et al.* 2015), and 1-butyl-2,3-dimethylimidazolium triflate ionic liquid (Kudo *et al.* 2011), were found capable of significantly increasing the LGO formation. In addition, the formation of FF can be selectively increased using acid catalysts such as $ZnCl_2$ (Lu *et al.* 2011a), $MgCl_2$ (Wan *et al.* 2009), H_2SO_4 (Branca *et al.* 2011), and $CuSO_4$/HZSM-5 (Zhang *et al*. 2014). However, very limited reports are available that deal with the selective production of other anhydrosugar and furan compounds.

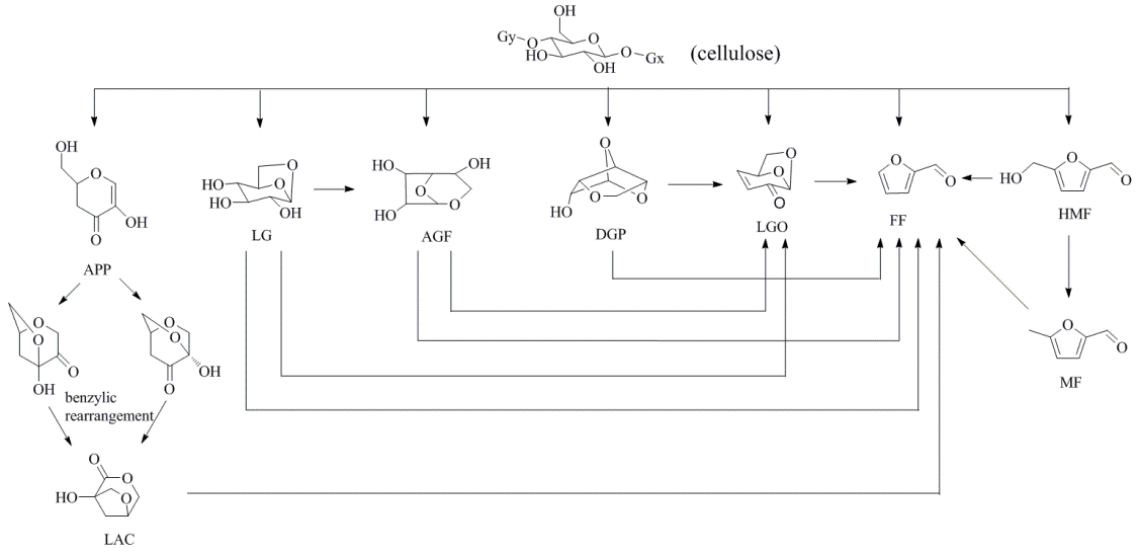

Fig. 1. The pyrolytic formation of anhydrosugar and furan products from cellulose

LAC is a valuable anhydrosugar derivative, containing a tetrahydrofuran ring and two chiral centers. The special lactone unit makes the LAC a potential building block for organic synthesis. It can be used to prepare various bioproducts, such as amide (Fabbri *et al.* 2007b), amino acid (Defant *et al.* 2011), muscarine-like compounds (Defant *et al.* 2015), and polyesters (Dobrzynski *et al.* 2009), *etc*. The LAC was first identified by Furneaux *et al.* (1988), who proposed that the LAC was derived from APP through a benzylic acid-type rearrangement reaction, while APP was produced *via* two sequential eliminations of the glucosidic substituents (Shafizadeh *et al.* 1978), as shown in Fig. 1.

Furneaux *et al.* (1988) also pointed out that the production of LAC could be increased from the pyrolysis of cellulose in the presence of certain Lewis acids, but not in the presence of protic acids. Fabbri *et al.* (2007a,b) further confirmed the structure of LAC and found a way to selectively produce LAC *via* the catalytic pyrolysis of cellulose in the presence of the nanopowder aluminium titanate (NP AlTi). Additionally, the same research group further reported that Sn-MCM-41 and Zr-MCM-41 could also be promising catalysts for selective LAC production (Torri *et al.* 2009a,b). They found that incorporation of Sn (IV) and Zr (IV) on the MCM-41 led to the formation of Lewis acid sites, which facilitated the LAC formation. Furthermore, Rutkowski (2012) found that the montmorillonite K-10

catalyst also possessed a certain ability to promote LAC formation. Recently, Mancini *et al.* (2014) performed the catalytic pyrolysis of cellulose, using the previously reported catalysts (Sn-MCM-41, montmorillonite K-10, and nanopowder aluminium titanate) to produce LAC-rich bio-oils and then quantitatively determined the LAC yields using ^{1}H NMR and FT-IR techniques. The highest LAC yield was 7.6 wt.%, obtained using the Sn-MCM-41 catalyst.

In this study, zinc-aluminium layered double oxide (Zn-Al-LDO) was considered as another promising catalyst for the selective production of LAC from cellulose. An analytical Py-GC/MS instrument was employed for the catalytic fast pyrolysis of cellulose and for the on-line analysis of the pyrolysis vapors. First, Zn-Al-LDO catalysts with various Zn/Al molar ratios were evaluated and compared for a determination of which yielded the highest LAC production. Then, to determine the optimal reaction condition for LAC production, several experiments were performed under various pyrolysis temperatures and catalyst-to-cellulose ratios. In addition, the catalyst montmorillonite K-10, which has been previously reported to be an effective catalyst for the production of LAC, was employed as a reference catalyst to be compared against the catalyst Zn-Al-LDO in terms of catalytic capability.

EXPERIMENTAL

Materials

The feedstocks used in this study were cellulose (Avicel PH-101), montmorillonite K-10 (>95%), zinc nitrate (99%), aluminium nitrate (99%), and aqueous ammonia (25 wt.%). The cellulose was purchased from Sigma (USA) and dried at 85 °C for 4 h before use in the experiments. The other materials were purchased from Aladdin Company (China).

Methods

Preparation and characterization of catalysts

Zinc-aluminium layered double hydroxides (Zn-Al-LDHs) were prepared using the co-precipitation method (Linares *et al.* 2015). First, zinc nitrate and aluminium nitrate were dissolved in deionized water at four different concentrations, producing four solutions with different Zn/Al molar ratios (R=1, 2, 3, or 4). Each solution was slowly added into a beaker, and the pH was maintained at approximately 10 by the addition of aqueous ammonia (25 wt.%). The slurries were stirred for 4 h and then kept in a water bath for 24 h at 60 °C. Afterwards, the precipitates were filtered and washed several times with deionized water. The resulting solids were dried at 80 °C for 12 h to obtain the Zn-Al-LDHs. Finally, the Zn-Al-LDHs were calcined at 500 °C for 5 h to obtain the Zn-Al-LDO catalysts. In acknowledgment of the different Zn/Al ratios, the four LDO catalysts were referred to as Zn-Al-LDO-1, Zn-Al-LDO-2, Zn-Al-LDO-3, and Zn-Al-LDO-4, respectively.

X-ray diffraction (XRD) analysis was conducted with a Rigaku Rotaflex diffractometer (Japan) equipped with Cu Kα radiation (λ=0.15406 nm). The data were recorded over the 2θ range of 5 to 70°. The crystalline phases were identified by comparison with the reference data from the files of the International Center for Diffraction Data (ICDD).

Nitrogen adsorption/desorption isotherms at 77 K were measured using an Autosorb-iQ-MP physisorption analyzer (Quantachrome, USA). The surface area was determined using the Brunauer-Emmett-Teller (BET) method. The pore volume and average pore diameter were determined by the Barrett-Joyner-Halenda (BJH) method.

The total acid sites of the four Zn-Al-LDO catalysts were determined by NH_3 temperature-programmed desorption (TPD) using a ChemBET Pulsar TPR/TPD analyzer (USA) with an on-line thermal conductivity detector (TCD). The detailed operation process can be seen in our previous study (Zhang *et al.* 2015). The TCD was firstly calibrated by the known amounts of NH_3, and thus, the total acid sites of the four Zn-Al-LDO catalysts can be calculated based on the measured NH_3 desorbed from the catalyst sample by the TCD.

Analytical Py-GC/MS experiments

The analytical Py-GC/MS experiments were conducted using a CDS Pyroprobe 5200HP pyrolyser (CDS Analytical, USA) connected to a Perkin Elmer GC/MS (Clarus 560; USA). The catalytic experiments were conducted within the *in situ* catalytic pattern. The experimental samples were prepared by mechanically mixing the cellulose and catalyst together in the middle of a quartz tube. Some quartz wool was placed at both sides of the cellulose/catalyst mixture, not only to immobilize the feedstock but also to prevent the escape of the solid particles during the pyrolysis process. The details of the experimental sample preparation can be found elsewhere (Zhang *et al.* 2015). In each experimental sample, the cellulose quantity was restricted to 0.20 mg, while the catalyst quantities were varied to achieve catalyst-to-cellulose ratios of 1, 2, 4, 6, and 8. Pure cellulose samples without a catalyst were also prepared for the experiments. An analytical balance with a readability of 0.01 mg was used for weighing.

The pyrolysis experiments were carried out at six temperatures, namely 290, 320, 350, 400, 450, and 500 °C, with a heating time of 20 s and heating rate of 20 °C/ms. The pyrolysis vapors were directly transformed into GC/MS. The GC oven was heated from 40 °C directly to 280 °C (2 min) at a heating rate of 15°C/min. The other details of the parameters of the GC/MS can be seen in a previous study (Zhang *et al.* 2015). The chromatographic peaks were identified using data from the NIST Library, Wiley Library, and based on the findings of a previous study (Fabbri *et al.* 2007a).

For each sample, the experiment was conducted at least three times to confirm the reproducibility of the pyrolytic product distributions. The analytical Py-GC/MS technique was not able to provide direct quantitative analysis of the products. The actual yields of the pyrolytic products can usually be determined *via* the external calibration method utilizing standard chemicals. However, pure LAC is not commercially available; thus, the LAC yields under various reaction conditions were unable to be determined. Despite the lack of quantitative determination, it is known that the chromatographic peak area of a compound varies linearly with its quantity and that the peak area percentage varies linearly with its concentration (Lu *et al.* 2012). Therefore, for each product, the change in yield could be determined by comparing the average peak area values obtained under different reaction conditions, and the changes in concentration among the detected compounds could be determined by comparing its peak area percentage values.

RESULTS AND DISCUSSION

Catalyst Properties

Figure 2 shows the XRD patterns of the Zn-Al-LDHs (before calcination) and the Zn-Al-LDOs (after calcination) with various Zn/Al molar ratios (R values). The XRD results of Zn-Al-LDHs were in agreement with those found for the hydrotalcite-like compounds (Hudson *et al.* 1995). During the calcination process, the layered structures were destroyed because of the removal of structural water from the interlayers (Guo *et al.* 2002). As a result, the ZnO, Al_2O_3, or $ZnAl_2O_4$ phases were formed. The Zn-Al-LDO-1 catalyst primarily consisted of Al_2O_3 and $ZnAl_2O_4$ phases. The Zn-Al-LDO-2, Zn-Al-LDO-3, and Zn-Al-LDO-4 catalysts primarily consisted of ZnO and $ZnAl_2O_4$ phases, and ZnO was predominant in the mixed phases, which agreed well with the results from a previous study (Guo *et al.* 2002). The absence of the Al_2O_3 phase in the Zn-Al-LDO-2, Zn-Al-LDO-3, and Zn-Al-LDO-4 catalysts was due to excess Zn^{2+}. Table 1 gives the textural properties and acidity of the four LDO catalysts. The BET surface areas of the Zn-Al-LDO-2, Zn-Al-LDO-3, and Zn-Al-LDO-4 catalysts were similar, but lower than that of the Zn-Al-LDO-1 catalyst. The average pore diameters of the Zn-Al-LDO-2 and Zn-Al-LDO-3 catalysts were obviously higher than those of the other two catalysts. The different textural properties of the LDO catalysts should be attributed to their different microstructures and contents of the $ZnAl_2O_4$, ZnO and Al_2O_3 (Zou *et al.* 2006). In addition, the acid sites of the four catalysts decreased along with the rising of the Zn/Al molar ratio.

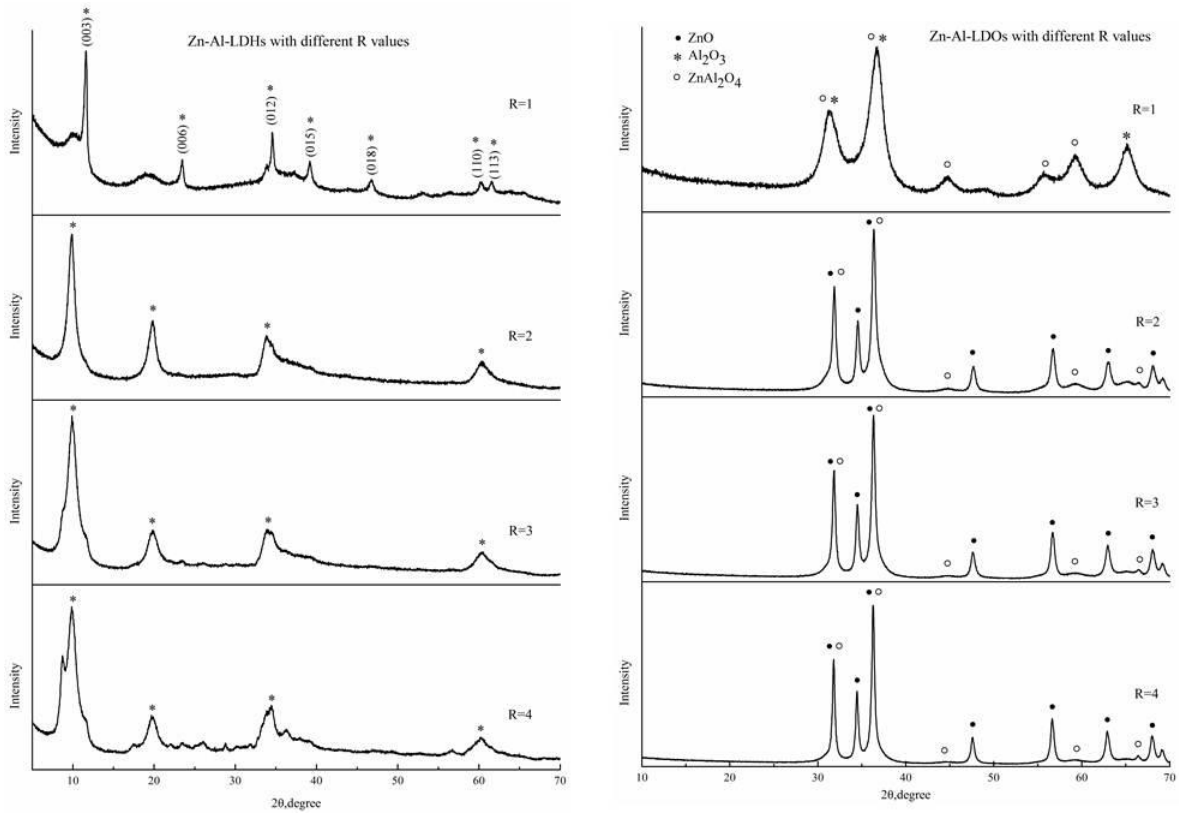

Fig. 2. XRD patterns of the Zn-Al-LDHs and Zn-Al-LDOs with various Zn/Al molar ratios

Table 1. Textural Properties and Acidity of the Zn-Al-LDO Catalysts

Zn/Al ratios (R ratios)	1	2	3	4
BET surface area (m^2/g)	112	62	61	60
Pore volume (cm^3/g)	0.2	0.2	0.2	0.3
Average pore diameter (nm)	3.4	9.5	11.3	3.8
Acid sites (mmol/g)	0.47	0.38	0.36	0.25

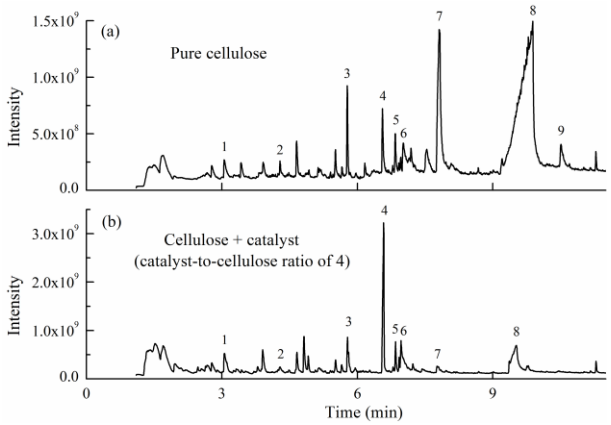

Fig. 3. Typical ion chromatograms from: (a) non-catalytic fast pyrolysis of cellulose at 350 °C and (b) catalytic fast pyrolysis of cellulose using Zn-Al-LDO-2 catalyst at 350 °C: (1) FF; (2) MF; (3) LGO; (4) LAC; (5) DGP; (6) HMF; (7) APP; (8) LG; and (9) AGF

Non-Catalytic and Catalytic Fast Pyrolysis of Cellulose

Fast pyrolysis of cellulose will produce water, organic volatile compounds and non-volatile oligosaccharides, which will be condensed to be liquid bio-oil. GC/MS is only able to determine the organic volatiles. It is notable that the GC-detectable compounds should account for the majority of the total organic compounds in bio-oil. The non-catalytic pyrolysis and catalytic fast pyrolysis of cellulose resulted in different pyrolytic product distributions. Figure 3(a) shows the typical ion chromatogram from the non-catalytic fast pyrolysis of cellulose at 350 °C. The low-temperature non-catalytic process produced various anhydrosugars (including LG, LAC, LGO, DGP, APP, and AGF), furans (HMF, MF, and FF), cyclopentanones, linear carbonyls, and other products. The major pyrolytic products, especially the anhydrosugars and furans, are numbered in Fig. 3. The LG was the predominant product, with the peak area percentage as high as 52.7%. The LAC was a very minor product, with its peak area percentage only 3.0%. More details of the pyrolytic product distribution and formation characteristics of the important products have been reported previously (Shen and Gu 2009; Lu *et al.* 2011b). In a previous study, it was confirmed that the formation of LAC was closely related to the APP, and specifically that their yields were inversely related, which meant that the formation of LAC would result in the decrease in APP (Lu *et al.* 2011b).

The pyrolytic product distribution changed greatly when the LDO catalyst was mechanically mixed with the cellulose, with the typical ion chromatogram shown in Fig. 3(b). The LG, APP, and a few other products decreased greatly, while the LAC increased remarkably and became the predominant product. As a result of the tendency of the LDO catalyst to promote LAC formation while inhibiting other competing pyrolytic products, a

LAC-rich liquid was obtained. As mentioned above, the LDO catalyst contained the $ZnAl_2O_4$, ZnO or Al_2O_3 phases. In order to further confirm the catalytic capability of the LDO catalyst, catalytic pyrolysis of cellulose with pure ZnO and Al_2O_3 were conducted and the results are shown in the Appendix (Fig. S1 and Table S1). It is seen that both the ZnO and Al_2O_3 possessed certain ability to increase the LAC formation, and the ZnO was more capable than the Al_2O_3. However, the LDO catalyst performed much better than the ZnO and Al_2O_3 on the enhancement of LAC production. Therefore, it can be inferred that the $ZnAl_2O_4$ phase was primarily responsible for the catalytic capacity for selective production of LAC.

Catalytic Pyrolytic Product Distributions under Different Conditions

Effects of catalysts with various Zn/Al molar ratios

The Zn/Al molar ratio has been shown to directly determine the composition of the LDO catalyst and thus affect its catalytic activities. Figure 4 shows the effects of the Zn/Al molar ratio on the total peak area of all detectable pyrolytic products as well as the peak area and peak area percentage of the three important products (LG, APP, and LAC). The results were obtained at the pyrolysis temperature of 350 °C and at the catalyst-to-biomass ratio of 4. Figure 4 also displays the results from the non-catalytic pyrolysis process and from the catalytic process, using the K-10 catalyst for comparison. Compared with its value under the non-catalytic process, under the K-10 catalysis the total peak area value decreased slightly, whereas under the LDO catalysis the value decreased remarkably. The result indicated that the catalytic pyrolysis by the LDO catalysts would obtain lower organic bio-oil yields than the catalytic pyrolysis by the K-10 catalyst.

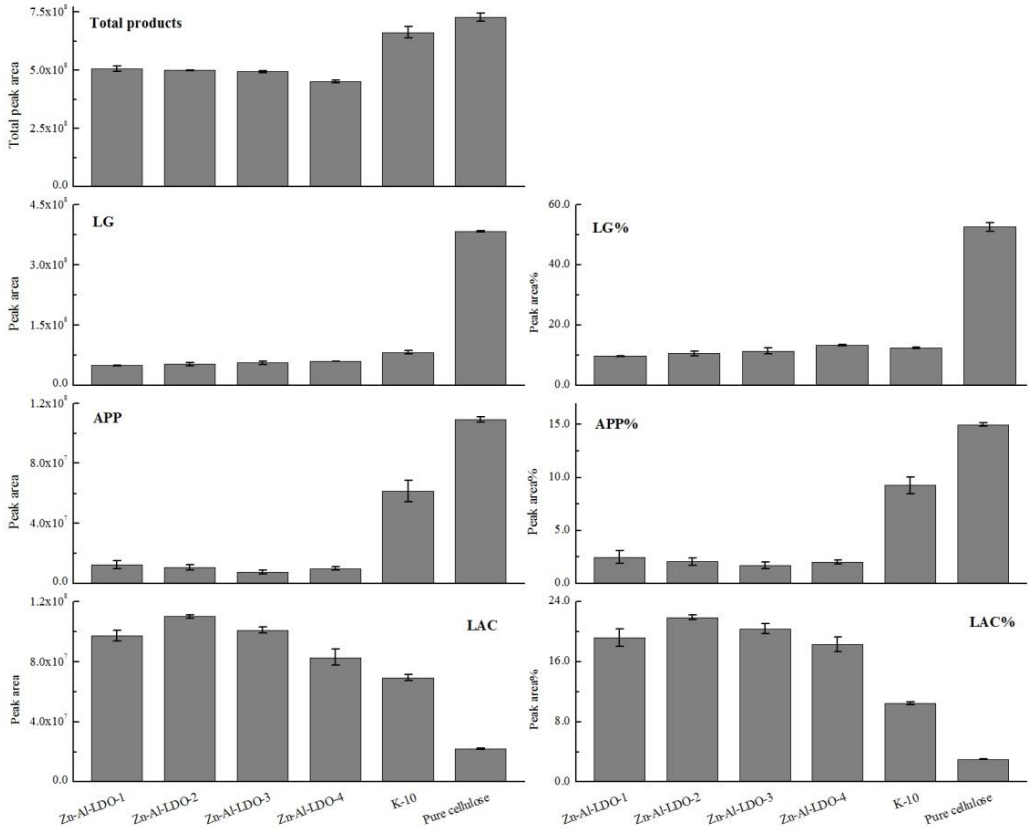

Fig. 4. Total peak area for all products as well as peak area and peak area percentage for LG, APP, and LAC from non-catalytic and catalytic fast pyrolysis of cellulose with different catalysts

With respect to LG, compared with non-catalytic process, both its yield (based on the peak area value) and concentration (based on the peak area percentage value) were obviously lower during the catalytic process. This phenomenon clearly indicated that the LDO catalyst could inhibit the formation of LG or cause the secondary conversion of LG, which was in agreement with a previous study that found the LG yield could be decreased by various metal oxide catalysts (Lu *et al.* 2010). In order to further confirm this point, the catalytic pyrolysis of pure LG was conducted and the results are shown in the Appendix (Fig. S2). The results clearly indicated that the pure LG was thermally stable during the non-catalytic pyrolysis process, but it could be easily converted into various light compounds under the Zn-Al-LDO catalyst. Moreover, the LG yields under the LDO catalysts were always lower than that under the K-10 catalyst. The APP was also noticeably decreased by the catalytic process, which could have been due to its secondary conversion to LAC.

Under all the Zn-Al-LDO catalysts, the LAC was greatly promoted by the catalytic process. All four Zn-Al-LDO catalysts performed much better than the K-10 catalyst to selectively produce the LAC, in terms of both yield and concentration. The peak area percentage of LAC produced from the Zn-Al-LDO-2 catalyst was 21.9%, compared with the value of 10.5% from the K-10 catalyst and only 3.0% from the non-catalytic process. Among the four Zn-Al-LDO catalysts, the catalyst with the Zn-Al molar ratio of 2 (Zn-Al-LDO-2) exhibited the best catalytic capacity towards the LAC, which might be due to the following reasons. Compared with the Zn-Al-LDO-3 and Zn-Al-LDO-4 catalysts, the Zn-Al-LDO-2 catalyst had higher $ZnAl_2O_4$ content, and the $ZnAl_2O_4$ was mainly responsible for the promoted LAC formation. In regard to the Zn-Al-LDO-1 and Zn-Al-LDO-2 catalysts, the Zn-Al-LDO-1 catalyst mainly consisted of $ZnAl_2O_4$ and Al_2O_3 phases, while the Zn-Al-LDO-2 catalyst mainly consisted of $ZnAl_2O_4$ and ZnO phases. As revealed above, the ZnO was more capable than the Al_2O_3 on the LAC production, and thus, the Zn-Al-LDO-2 catalyst performed better than the Zn-Al-LDO-1 catalyst to selectively produce the LAC. For this reason, the following studies, the Zn-Al-LDO-2 catalyst was employed for further investigation of the effects of various reaction conditions on selective LAC production.

Effects of pyrolysis temperature

The pyrolysis temperature is an important factor influencing the product distribution of the reaction. Figure 5 shows the effects of the pyrolysis temperature on total product peak area as well as the peak area and peak area percentage of LG and LAC from both non-catalytic and catalytic pyrolysis processes. The catalytic experiments were all conducted under the catalyst-to-cellulose ratio of 4. According to Fig. 5, during both non-catalytic and catalytic processes, the total product yield increased monotonically with increasing pyrolysis temperature, which was thought to be due to the temperature-promoted pyrolysis reactions (Lu *et al.* 2011b). Moreover, the catalytic processes always obtained lower total product yields than those of non-catalytic processes, because the LDO catalysts possessed strong ability to inhibit the devolatilization of cellulose.

During the non-catalytic process, the yields of LG and LAC increased monotonically with increasing pyrolysis temperature, although their concentrations were not greatly affected by the pyrolysis temperature (Lu *et al.* 2011b). During the catalytic process, the LG yield also increased along with the pyrolysis temperature, but was always lower than that from the non-catalytic process. Meanwhile, with the increase in temperature, the concentration of LG decreased very rapidly initially, from 55.8% at 290 °C to 10.6%

at 350 °C, and then increased to 27.2% by 500 °C. These results indicated that the LDO catalyst was most effective at inhibiting LG formation at 350 °C. With respect to the LAC, both its yield and concentration increased greatly from 290 to 350 °C, but at higher temperatures gradually decreased. The peak area percentage values of the LG and LAC were inversely related, which indicated the competitiveness between the two products. Generally, 350 °C was the temperature most favorable for the formation of LAC during the catalytic process, while at higher and lower pyrolysis temperatures, its formation was less prevalent than the formation of LG.

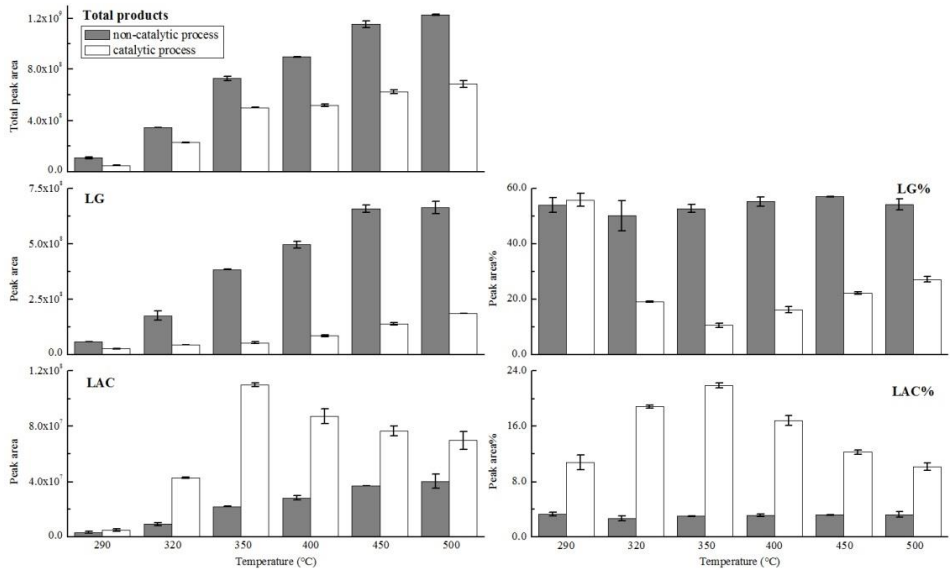

Fig. 5. Total peak area for all products as well as peak area and peak area percentage for LG and LAC under various pyrolysis temperatures

Effects of catalyst-to-cellulose ratio

Further experiments were conducted to determine the effects of the catalyst-to-cellulose ratio on the pyrolytic product distribution at the reaction temperature of 350 °C. Figure 6 shows the changes in total pyrolytic products and major anhydrosugars, including LAC, LG, APP, LGO, DGP, and AGF, under various catalyst-to-cellulose ratios. Figure 7 shows the results for the furan compounds, including FF, MF, and HMF. According to Fig. 6, the total product yield decreased monotonously as a function of the increase in catalyst-to-cellulose ratio. This could be attributed to the following two reasons. First, the presence of the catalyst could have inhibited the devolatilization of cellulose or caused the secondary cracking of primary pyrolytic products into permanent gases, resulting in decreased organic product yield. Second, an excess quantity of the catalyst could have increased resistance to the heat and mass transfer (Mullen and Boateng 2010), which would have inhibited the formation of pyrolytic products. In terms of LAC, its yield and concentration increased initially and later decreased, with the maximal values obtained at the catalyst-to-cellulose ratio of 4. Based on the peak area percentage results, it can be seen that the formation of LAC was sensitive to the catalyst-to-cellulose ratio. Neither a low nor high catalyst-to-cellulose ratio was favorable for LAC formation.

It is necessary to note that during the analytical catalytic pyrolysis experiments, the cellulose/catalyst mixtures were kept motionless. The contact between the cellulose and catalyst was limited, and thus, the sufficient catalytic pyrolysis required relatively high catalyst quantity. On the other hand, during the industrial catalytic pyrolysis process, it can

be inferred that less catalyst should be required, since the pyrolysis reactor (such as the fluidizing bed-based pyrolysis reactor) can ensure the good mixing and contact between the cellulose and catalyst. Furthermore, the LDO catalyst is thermally stable, and can be recycled in industrial pyrolysis process. All these facts will ensure the economic feasibility of this technique.

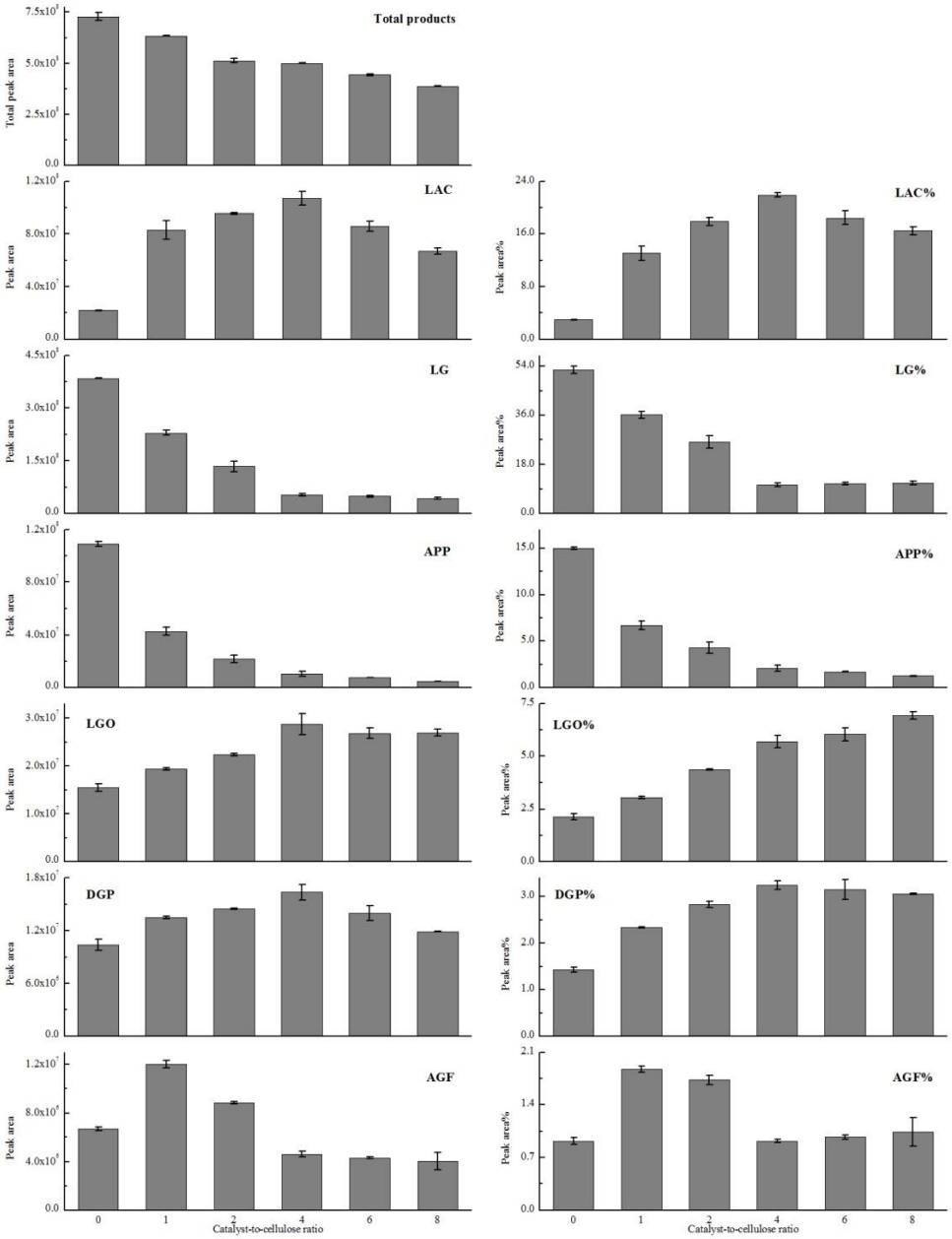

Fig. 6. Total peak area for all products as well as peak area and peak area percentage for LAC, LG, APP, LGO, and AGF under various catalyst-to-cellulose ratios

With respect to the anhydrosugar and furan compounds, these were formed in competing pyrolytic pathways; moreover, certain compounds could be derived from the secondary conversion of other compounds, as shown in Fig. 1. According to Figs. 6 and 7, these compounds exhibited different formation characteristics and could be classified into three groups based on these differences. The first group included LG and APP, both of

whose yields and concentrations decreased monotonically along with the increase in catalyst-to-cellulose ratio. The second group included LAC, DGP, AGF, and HMF, whose yields and concentrations increased initially and then decreased along with the increase in catalyst-to-cellulose ratio. The third group included LGO, FF, and MF, whose yields increased initially and then remained relatively stable while their concentrations increased monotonically. These phenomena could be attributed to the different degrees of competitiveness among the pyrolytic pathways for the formation of these products under different catalyst quantities, and also to their secondary conversions.

For the two products of the first group, APP was the precursor of the LAC and was easily converted into LAC during the catalytic process (Furneaux *et al.* 1988). Thus, its yield decreased greatly with the increase in the catalyst-to-cellulose ratio. In addition, the LG formation pathway was inhibited by the LDO catalyst and the formed LG also underwent a secondary cracking reaction during the catalytic process. Hence, the LG yield decreased markedly with the increase in catalyst quantity. As a result of the inhibited LG formation, the other competing pyrolytic pathways were enhanced, resulting in the increased formation of various other anhydrosugar and furan products, *i.e.*, the products of the second and third groups.

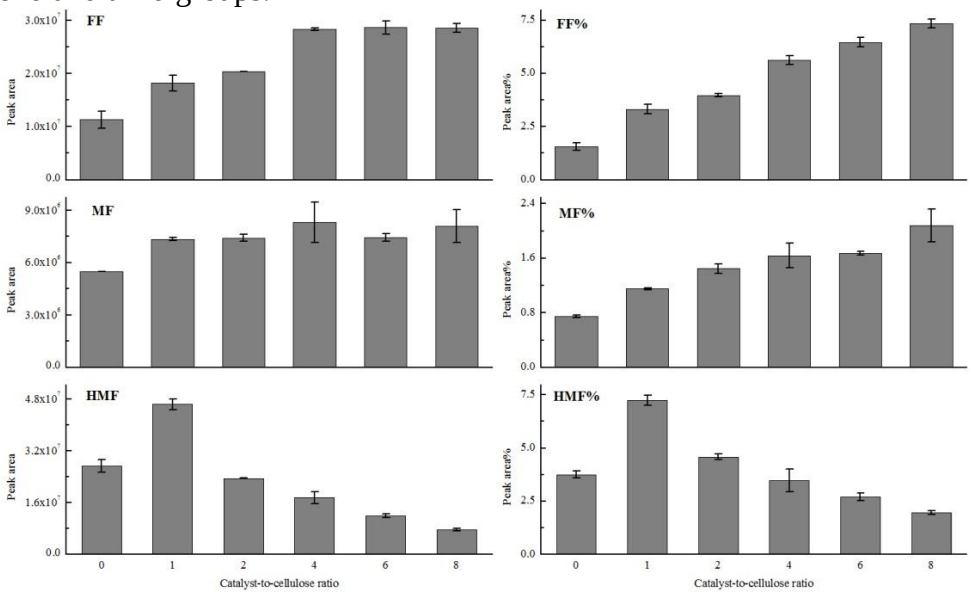

Fig. 7. Peak area and peak area percentage for FF, MF, and HMF under various catalyst-to-cellulose ratios

With respect to the four products of the second group, AGF and HMF were increased only at low catalyst-to-cellulose ratios, while the LAC and DGP were favored at medium catalyst quantities. These characteristics suggested that the formation pathways of the four compounds were favorable only at low or medium catalyst quantities and that the four compounds underwent remarkable secondary cracking reactions, especially at high catalyst quantities. Previous studies have confirmed that these compounds are converted to more stable compounds, such as LGO and FF, during the acid-catalyzed pyrolysis process (Lin *et al.* 2009; Torri *et al.* 2009a; Zhang *et al.* 2015). To further confirm this point, both non-catalytic and catalytic pyrolysis reactions of pure HMF were performed, and the results are shown in the Appendix (Fig. S3). Pure HMF was thermally stable, only forming a small amount of MF and 2,5-furandicarboxaldehyde during the non-catalytic process. However,

in the presence of the LDO catalyst, the HMF would be easily converted, which clearly explained the above result of the decreased HMF yield at high catalyst-to-cellulose ratios.

In the case of the three products of the third group (LGO, FF, and MF), their formation was favored at high catalyst-to-cellulose ratios, which could be partly attributed to the secondary cracking of certain primary products to form the three products. As indicated in Fig. S3, the MF could have been obtained from the cracking of the HMF. In addition, previous studies have indicated that LGO could be derived from the activities of LG, DGP, and AGF in the presence of acid catalysts (Lin *et al.* 2009; Torri *et al.* 2009a). The FF could have been produced by almost all of the above anhydrosugars and furans (LG, AGF, DGP, LGO, LAC, HMF, and MF) under acid catalytic processes.

Based on the above results, although the LDO catalyst was able to promote the formation of several pyrolytic products, the yield of LAC increased much more than those of the other products, which allowed for selective LAC production from the LDO-catalyzed pyrolysis process. However, the selectivity of the LAC was sensitive to the pyrolysis temperature and catalyst-to-cellulose ratio; thus, it was deemed essential for LAC production to carefully control the pyrolysis conditions.

CONCLUSIONS

1. The fast pyrolysis of cellulose mechanically mixed with the Zn-Al-LDO catalyst offers a way to selectively produce LAC. The Zn-Al-LDO catalyst possessed the catalytic capability to inhibit the formation of LG and to promote the formation of LAC and some other products (LGO, DGP, MF, and FF).
2. Both pyrolysis temperature and catalyst-to-cellulose ratio played important roles in LAC formation. The LAC yield and concentration increased initially and then decreased with increasing pyrolysis temperature and catalyst-to-cellulose ratio.
3. The LDO catalyst with a Zn/Al molar ratio of 2 exhibited the best capacity for producing LAC. The maximal LAC yield was obtained at 350 °C and at the catalyst-to-cellulose ratio of 4, and resulted in a peak area percentage of 21.9% (calculated from GC/MS data), compared with the peak area percentage of only 3.0% for the non-catalytic process.
4. The LDO catalyst performed better than the previously reported montmorillonite K-10 catalyst on the promotion of LAC production.

ACKNOWLEDGMENTS

The authors thank the National Natural Science Foundation of China (51276062), the National Basic Research Program of China (2015CB251501), the 111 Project (B12034), the Foundation of State Key Laboratory of Coal Combustion (FSKLCC1413), and the Fundamental Research Funds for the Central Universities (2014ZD17, 2015ZZD02, 2015XS60) for financial support.

REFERENCES CITED

Branca, C., Galgano, A., Blasi, C., Esposito, M., and Di Blasi, C. (2011). "H_2SO_4-catalyzed pyrolysis of corncobs," *Energ. Fuel* 25(1), 359-369. DOI: 10.1021/ef101317f

Defant, A., Mancini, I., Torri, C., Malferrari, D., and Fabbri, D. (2011). "An efficient route towards a new branched tetrahydrofurane d-sugar amino acid from a pyrolysis product of cellulose," *Amino Acids* 40(2), 633-640. DOI: 10.1007/s00726-010-0690-4

Defant, A., Mancini, I., Matucci, R., Bellucci, C., Dosi, F., Malferrari, D., and Fabbri, D. (2015). "Muscarine-like compounds derived from a pyrolysis product of cellulose," *Org. Biomol. Chem.* 13(22), 6291-6298. DOI: 10.1039/c5ob00339c

Dobrzynski, P., Fabbri, D., Torri, C., Kasperczyk, J., Kaczmarczyk, B., and Pastusiak, M. (2009). "A novel hydroxy functionalized polyester obtained by ring opening copolymerization of L-lactide with a pyrolysis product of cellulose," *J. Polym. Sci. Part. A.* 47(1), 247-257. DOI: 10.1002/pola.23149

Dobele, G., Dizhbite, T., Rossinskaja, G., Telysheva, G., Meier, D., Radtke, S., and Faix, O. (2003). "Pre-treatment of biomass with phosphoric acid prior to fast pyrolysis: A promising method for obtaining 1,6-anhydrosaccharides in high yields," *J. Anal. Appl. Pyrol.* 68, 197-211. DOI: 10.1016/S0165-2370(03)00063-9

Fabbri, D., Torri, C., and Baravelli, V. (2007a). "Effect of zeolites and nanopowder metal oxides on the distribution of chiral anhydrosugars evolved from pyrolysis of cellulose: An analytical study," *J. Anal. Appl. Pyrol.* 80(1), 24-29. DOI: 10.1016/j.jaap.2006.12.025

Fabbri, D., Torri, C., and Mancini, I. (2007b). "Pyrolysis of cellulose catalysed by nanopowder metal oxides: Production and characterisation of a chiral hydroxylactone and its role as building block," *Green Chem.* 9(12), 1374-1379. DOI: 10.1039/B707943E

Furneaux, R. H., Mason, J. M., and Miller, I. J. (1988). "A novel hydroxylactone from the Lewis acid catalysed pyrolysis of cellulose," *J. Chem. Soc. Perkin Trans.* 1(1), 49-51. DOI: 10.1039/P19880000049

Guo, Y. H., Li, D. F., Hu, C. W., Wang, E. B., Zou, Y. C., Ding, H., and Feng, S. H. (2002). "Preparation and photocatalytic behavior of Zn/Al/W(Mn) mixed oxides via polyoxometalates intercalated layered double hydroxides," *Micropor. Mesopor. Mater.* 56(2), 153-162. DOI: 10.1016/S1387-1811(02)00481-X

Hudson, M. J., Carlino, S., and Apperley, D. C. (1995). "Thermal conversion of a layered (Mg/Al) double hydroxide to the oxide," *J. Mater. Chem.* 5(2), 323-329. DOI: 10.1039/jm9950500323

Kudo, S., Zhou, Z. W., Norinaga, K., and Hayashi, J. (2011). "Efficient levoglucosenone production by catalytic pyrolysis of cellulose mixed with ionic liquid," *Green Chem.* 13(11), 3306-3311. DOI: 10.1039/c1gc15975e

Lin, Y. C., Cho, J., Tompsett, G. A., Westmoreland, P. R., and Huber, G. W. (2009). "Kinetics and mechanism of cellulose pyrolysis," *J. Phys. Chem. C* 113(46), 20097-20107. DOI: 10.1021/jp906702p

Linares, C. F., Vásquez, M., Castillo, R., Bretto, P., Solano, R., and Rincón, A. (2015). "Applications of CoMo/calcined quaternary hydrotalcites for hydrotreatment reactions," *Fuel Process. Technol.* 132, 105-110. DOI: 10.1016/j.fuproc.2014.12.043

Liu, C. J., Wang, H. M., Karim, A. M., Sun, J. M., and Wang, Y. (2014). "Catalytic fast pyrolysis of lignocellulosic biomass," *Chem. Soc. Rev.* 43(22), 7594-7623. DOI: 10.1039/C3CS60414D

Lu, Q., Zhang, Z. F., Dong, C. Q., and Zhu, X. F. (2010). "Catalytic upgrading of biomass fast pyrolysis vapors with nano metal oxides: An analytical Py-GC/MS study," *Energies* 3(11), 1805-1820. DOI: 10.3390/en3111805

Lu, Q., Dong, C. Q., Zhang, X. M., Tian, H. Y., Yang, Y. P, and Zhu, X. F. (2011a). "Selective fast pyrolysis of biomass impregnated with $ZnCl_2$ to produce furfural: Analytical Py-GC/MS study," *J. Anal. Appl. Pyrol.* 90(2), 204-212. DOI: 10.1016/j.jaap.2010.12.007

Lu, Q., Yang, X. C., Dong, C. Q., Zhang, Z. F., Zhang, X. M., and Zhu, X. F. (2011b). "Influence of pyrolysis temperature and time on the cellulose fast pyrolysis products: Analytical Py-GC/MS study," *J. Anal. Appl. Pyrol.* 92(2), 430-438. DOI: 10.1016/j.jaap.2011.08.006

Lu, Q., Zhang, X. M., Zhang, Z. B., Zhang, Y., Zhu, X. F., and Dong, C. Q. (2012). "Catalytic fast pyrolysis of cellulose mixed with sulfated titania to produce levoglucosenone: Analytical Py-GC/MS study," *BioResources* 7(3), 2820-2834. DOI: 10.15376/biores.7.3.2820-2834

Mancini, I., Dosi, F., Defant, A., Crea, F., and Miotello, A. (2014). "Upgraded production of (1R,5S)-1-hydroxy-3,6-dioxa-bicyclo[3.2.1]octan-2-one from cellulose catalytic pyrolysis and its detection in bio-oils by spectroscopic methods," *J. Anal. Appl. Pyrol.* 110, 285-290. DOI: 10.1016/j.jaap.2014.09.014

Mullen, C. A., and Boateng, A. A. (2010). "Catalytic pyrolysis-GC/MS of lignin from several sources," *Fuel Process. Technol.* 91(11), 91-99. DOI: 10.1016/j.fuproc.2010.05.022

Rutkowski, P. (2012). "Pyrolytic behavior of cellulose in presence of montmorillonite K10 as catalyst," *J. Anal. Appl. Pyrol.* 98, 115-122. DOI: 10.1016/j.jaap.2012.07.012

Shafizadeh, F., Furneaux, R. H., Stevenson, T. T., and Cochran, T. G. (1978). "1,5-anhydro-4-deoxy-d-glycero-hex-1-en-3-ulose and other pyrolysis products of cellulose," *Carbohydr. Res.* 67(2), 433-447. DOI: 10.1016/S0008-6215(00)84131-2

Shen, D. K., and Gu, S. (2009). "The mechanism for thermal decomposition of cellulose and its main products," *Bioresour. Technol.* 100(24), 6496-6504. DOI: 10.1016/j.biortech.2009.06.095

Sui, X. W., Wang, Z., Liao, B., Zhang, Y., and Guo, Q. X. (2012). "Preparation of levoglucosenone through sulfuric acid promoted pyrolysis of bagasse at low temperature," *Bioresour. Technol.* 103(1), 466-469. DOI: 10.1016/j.biortech.2011.10.010

Torri, C., Lesci, I. G., and Fabbri, D. (2009a). "Analytical study on the production of a hydroxylactone from catalytic pyrolysis of carbohydrates with nanopowder aluminium titanate," *J. Anal. Appl. Pyrol.* 84(1), 25-30. DOI: 10.1016/j.jaap.2008.10.002

Torri, C., Lesci, I. G., and Fabbri, D. (2009b). "Analytical study on the pyrolytic behaviour of cellulose in the presence of MCM-41 mesoporous materials," *J. Anal. Appl. Pyrol.* 85(1), 192-196. DOI: 10.1016/j.jaap.2008.11.024

Wan, Y. Q., Chen, P., Zhang, B., Yang, C. Y., Liu, Y. H., Lin, X. Y., and Ruan, R. (2009). "Microwave-assisted pyrolysis of biomass: Catalysts to improve product selectivity," *J. Anal. Appl. Pyrol.* 86(1), 161-167. DOI: 10.1016/j.jaap.2009.05.006

Zhang, H. Y., Liu, X. J., Lu, M. Z., Hu, Y. Y., Lu, L. G., Tian, X. N., and Ji, J. B. (2014). "Role of Brønsted acid in selective production of furfural in biomass pyrolysis," *Bioresour. Technol.* 169, 800-803. DOI: 10.1016/j. biortech. 2014.07.053

Zhang, Z. B., Lu, Q., Ye, X. N., Wang, T. P., Wang, X. H., and Dong, C. Q. (2015). "Selective production of levoglucosenone from catalytic fast pyrolysis of biomass mechanically mixed with solid phosphoric acid catalysts," *Bioenergy Res.* 8, 1263-1274. DOI: 10.1007/s12155-015-9581-6

Zhuang, X. L., Zhang, H. X., Yang, J. Z., and Qi, H. Y. (2001). "Preparation of levoglucosan by pyrolysis of cellulose and its citric acid fermentation," *Bioresour. Technol.* 79(1), 63-66. DOI: 10.1016/S0960-8524(01)00023-2

Zou, L., Li, F., Xiang, X., Evans, D. G., and Duan, X. (2006). "Self-generated template pathway to high-surface-area zinc aluminate spinel with mesopore network from a single-source inorganic precursor," *Chem. Mater.* 18(25), 5852-5859. DOI: 10.1021/cm0606124

Article submitted: June 26, 2015; Peer review completed: August 11, 2015; Revised version received: October 11, 2015; Accepted: October 13, 2015; Published: October 28, 2015.
DOI: 10.15376/biores.10.4.8295-8311

APPENDIX

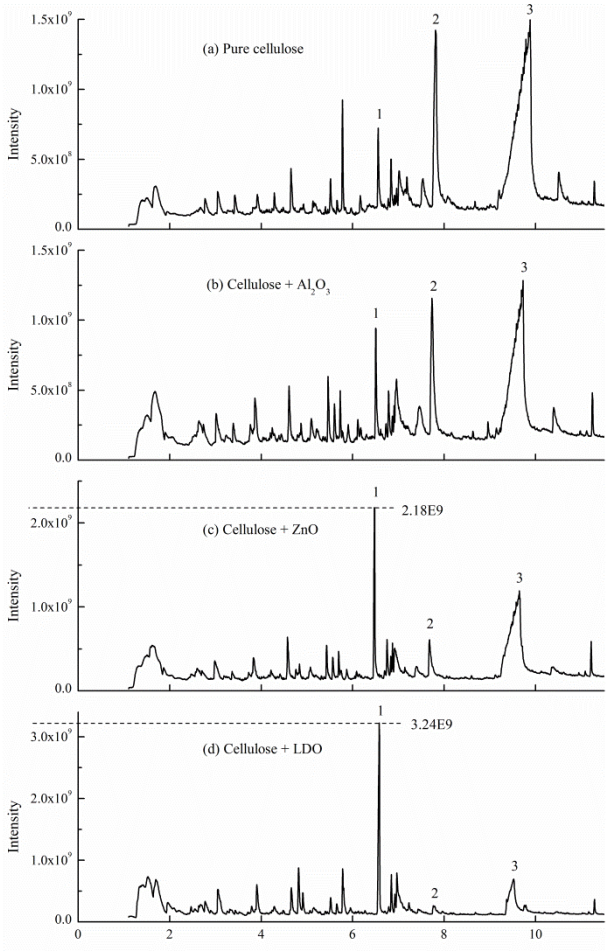

Fig. S1. Typical ion chromatograms from: (a) non-catalytic fast pyrolysis of cellulose at 350 °C; (b) catalytic fast pyrolysis of cellulose using Al_2O_3 catalyst at 350 °C; (c) catalytic fast pyrolysis of cellulose using ZnO catalyst at 350 °C; (d) catalytic fast pyrolysis of cellulose using Zn-Al-LDO-2 catalyst at 350 °C
(1) LAC; (2) APP; (3) LG
Note: Catalyst-to-cellulose ratio of 4 was employed in the above three catalytic pyrolysis experiments.

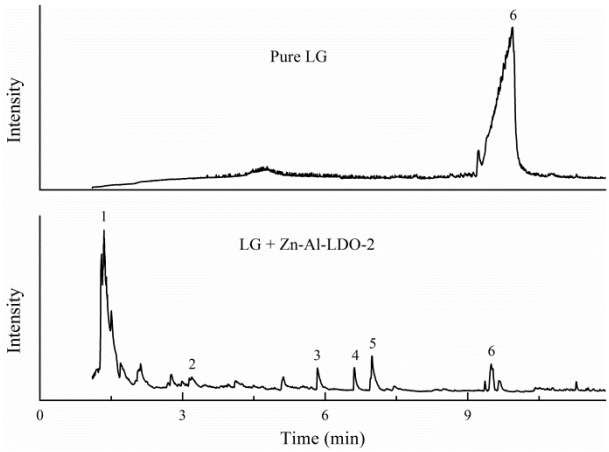

Fig. S2. Typical ion chromatograms from non-catalytic and catalytic fast pyrolysis of pure LG: (1) Gases; (2) FF; (3) LGO; (4) LAC; (5) 2,3-Anhydro-*D*-mannosan; (6) LG

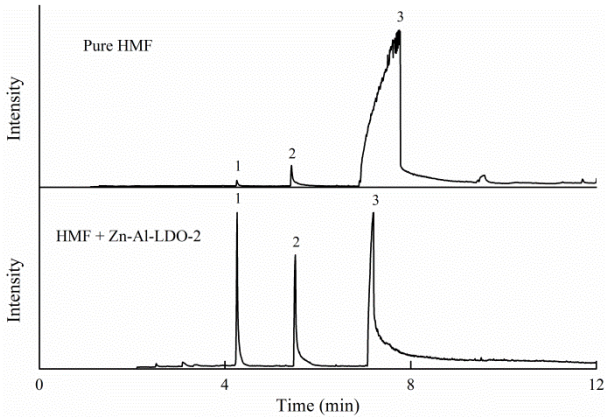

Fig. S3. Typical ion chromatograms from non-catalytic and catalytic fast pyrolysis of pure HMF: (1) MF; (2) 2,5-Furandicarboxaldehyde; (3) HMF

Table S1. Peak Area and Peak Area Percentage of LAC from Non-catalytic and Catalytic Pyrolysis of Cellulose using Different Catalysts (corresponding to **Fig. S1**)

	Pure cellulose	Cellulose+Al_2O_3	Cellulose+ZnO	Cellulose+LDO
Peak area	2.2E+07	2.5E+07	6.9E+07	1.1E+08
Peak area%	3.0	4.2	12.5	21.9